Light emitters and modulators on SOI for optical interconnects

Yikai Su*[a], Ciyuan Qiu[a], Yong Zhang[a, b], Ruili Liu[a]
[a] State Key Lab of Advanced Optical Communication Systems and Networks, Department of Electronic Engineering, Shanghai Jiao Tong University, Shanghai 200240, China
[b] Wuhan National Laboratory for Optoelectronics and School of Optical and Electronic information, Huazhong University of Science and Technology, Wuhan, Hubei, 430074, China

ABSTRACT

We discuss light emitters and modulators in silicon photonic interconnects. In particular, we experimentally demonstrate resonant luminescence from Ge quantum dots embedded in a photonic crystal ring resonator (PCRR) at room temperature. Six sharp resonant peaks are observed, which correspond to the resonant modes supported by the PCRR. We further study a high speed silicon-graphene nanobeam modulator, and a silicon spatial light modulator. These devices show great potential in future high density and high capacity interconnection systems.

Keywords: Light emitter, modulator, silicon photonics, interconnect

1. INTRODUCTION

In optical interconnections, multi-mode vertical cavity surface emitting laser (VCSEL) technology has dominated short reach links mainly due to its low cost, easy coupling, and high bandwidth density. Recently, mega data center offers an application scenario where high-performance integrated photonic devices show advantages in transmission distance over $\geqslant$300 m, high speed of $\geqslant$25 Gb/s, and more channel counts of $\geqslant$4 [1]. Silicon photonics, with its high index contrast nature, provides an effective approach to high density integration. Its CMOS compatible fabrication process may lower the cost in high volume. In addition, the interface to a silicon photonic device is single mode fiber, which is ideal for switching in mega data centers.

In this paper, we discuss light emitters and modulators in silicon photonic interconnects. Here we experimentally demonstrate resonant luminescence from Ge quantum dots embedded in a photonic crystal ring resonator (PCRR) at room temperature. We then study a high speed silicon-graphene nanobeam modulator, and a silicon spatial light modulator. These devices show great promise in future high density and high capacity interconnection systems.

2. LIGHT EMITTERS

Silicon based optical interconnect is now considered as a promising solution to overcome the limited bandwidth and high power consumption of traditional electric interconnects [2]. The realization of silicon based light source is still a major challenge due to the indirect band gap of bulk silicon. Many efforts have been made to solve this problem, including silicon nanocrystals [3], bulk crystalline silicon [4][5], optically active defects in crystalline Si [6], erbium doping in silicon [7], tensile-strained n-type Ge [8], III-V lasers [9] and so on. Among these candidates, Ge self-assembled quantum dots (QDs) have attracted much attention. The advantages of Ge QDs include: easy fabrication, light emission between 1.3-1.6 μm in the telecom band and compatibility with complementary metal-oxide semiconductor (CMOS) processes [10][11]. Considering poor spectral purity, low directionality and low luminescence intensity of light emission from Ge QDs, different microcavities were utilized to enhance light emission and select emission wavelength [12]-[16].

*yikaisu@sjtu.edu.cn; phone +86 21 3420 7924; fax +86 21 3420 4371
Part of the work performed by Yong Zhang was at Huazhong University of Science and Technology.

Optical Interconnects XVI, edited by Henning Schröder, Ray T. Chen, Proc. of SPIE Vol. 9753, 97530M

We demonstrate resonant luminescence from Ge QDs embedded in a photonic crystal ring resonantor (PCRR) at room temperature. Six sharp resonant peaks are observed in the PL spectrum of the PCRR, and the strongest resonant luminescence peak is located at 1542 nm. Three-dimensional finite-difference time-domain (3D-FDTD) method is applied to calculate the resonant modes for the PCRR and analyze the PL spectrum of the PCRR.

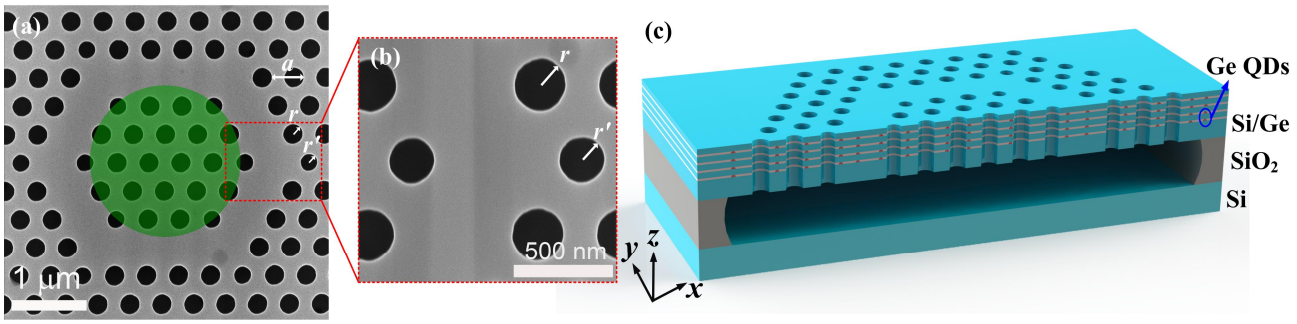

Fig. 1 (a) SEM image of fabricated PCRR embedded with Ge QDs. The excitation spot is shown with a green circle. (b) Magnified micrograph of the corner of the PCRR. The radius r′ of air holes at the corner of the PCRR is reduced by 15 nm. (c) Schematic structure of the device. The red dots represent Ge self-assembled QDs in the top Si/Ge layer. The BOX under the photonic crystal region is removed to form the freestanding structure.

The scanning electron microscope (SEM) images of fabricated PCRR structure is shown in Figs. 1(a) and (b). The ring resonator is formed by removing 20 air holes in shape of a hexagon. The schematic structure of the device is shown in Fig. 1(c). In the top Si/Ge layer, there are four layers of Ge self-assembled QDs, shown with red dots. The BOX under the photonic crystal region is removed to form the freestanding structure.

Figure 2(a) shows the room-temperature PL spectra for the sample, the power of the incident excitation laser is 16 μW. Red and black curves represent the PL spectrum of the PCRR and unprocessed Si/Ge membrane, respectively. Several sharp resonant peaks are observed to dominate the spectrum over an almost flat and weak background emission in the PL spectrum of the PCRR. There are clearly six sharp resonant emission peaks in the telecom wavelength range from 1500 to 1600 nm. Compared to the unprocessed membrane, the PL intensity from the PCRR is significantly enhanced at the resonant peaks. Figure 2(b) shows the magnified graph of the PL spectrum for the emission peak 4 of the PCRR. The wavelength of the peak 4 is 1542.58 nm, and the full-width-half-maximum (FWHM) is 0.5 nm obtained from Lorentz fitting. The corresponding Q factor is 3085.

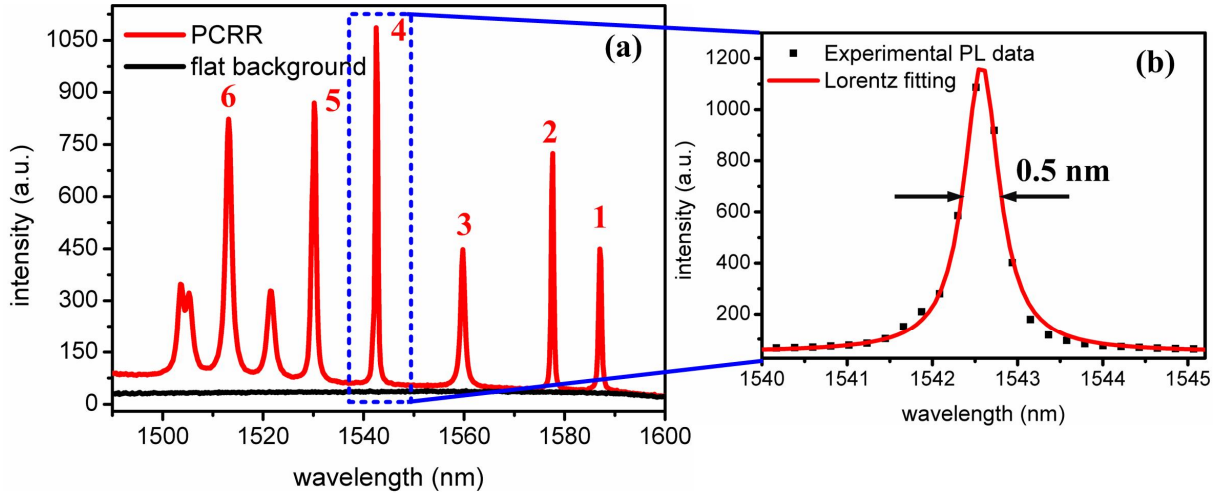

Fig. 2 (a) PL spectrum of the PCRR at room temperature at an excitation power of 16 μW. (b) the magnified graph of the PL spectrum for the emission peak 4 of the PCRR.

The photonic crystal cavity structure can be easily integrated into a lateral p-i-n junction for current injection [16]. The proposed compact device can achieve light emission in the telecom wavelength, which shows a possible way to realize CMOS-compatible silicon-based light emitters.

3. MODULATORS

A silicon EO modulator is an important component for enabling optical interconnection systems on a microelectronic chip. Several high-speed EO modulators based on free carrier dispersion effect have been demonstrated, including micro-ring modulator [17] and Mach–Zehnder modulator [18]. To achieve a speed at tens of GHz, PN junctions are embedded in these EO modulators and the free carriers in the silicon can be fast depleted. Since silicon has low nonlinear electro-optic effect [19], the devices have a relatively large footprint.

Graphene, a sheet of carbon atoms in a hexagonal lattice, has attracted great interest recently in nanoscale photonic circuit research [19]. By tuning its Fermi level through electric gating, its interband absorption can be controlled in the communication band. Since the graphene has ultrawide band tunability and ultrahigh electron mobility ~200000 $cm^2 V^{-1} s^{-1}$ [20], it is considered as a promising material to build active optoelectronic devices for high-speed communications. Many EO modulator based on silicon-graphene hybrid structure have been proposed and experimentally demonstrated, such as a silicon waveguide structure [20], a PhC cavity [21], and a micro-ring resonator [22] .

We propose two new types of EO modulators based on silicon-graphene hybrid structure, including a nanobeam modulator [23] and a micro-scale spatial light modulator valve [24]. The nanobeam EO modulator provides a large free spectral range (FSR) of 125.6 nm, a high modulation speed of 133 GHz, and a large modulation depth of ~12.5 dB which would be useful in DWDM optical communication systems. Furthermore, MSLV is built on 1D photonic crystal cavity and has a modulation speed up to 45 GHz which is two orders faster than the previous demonstrated silicon based MSLV [25].

3.1 Nanobeam modulator

Here we present a nanobeam modulator as shown in Fig.2. Fig. 2(a) shows the schematic perspective view of the proposed EO modulator. The nanobeam consists of three sections including one center taper section and two reflector sections which form a FP cavity. Detail device parameters can be found in [23]. Light travelling in the waveguide can be evanescently coupled into the nanobeam resonant cavity and there is no light output when the input light wavelength matches the resonant wavelength. This causes a notch in the transmission spectrum. Furthermore, the nanobeam resonant cavity has a relatively large FSR and has single resonant wavelength in the communication band.

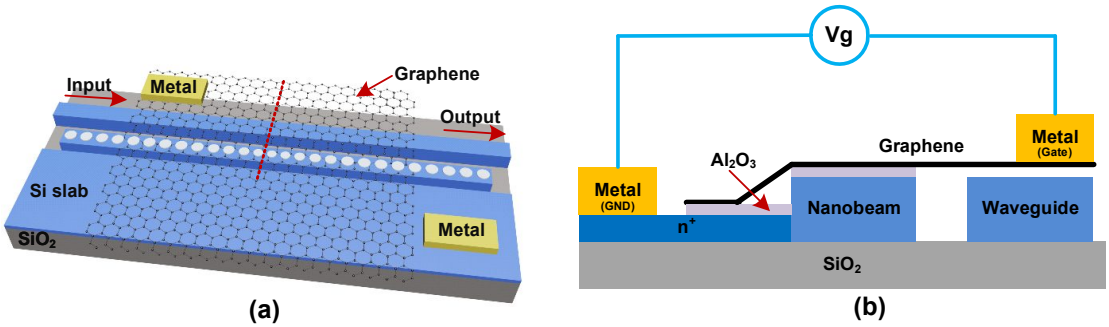

Figure.2 (a) Schematic perspective view of the proposed EO modulator. Note that there is no graphene covering the air holes of the PCN cavity. (b) The cross-section of the proposed device corresponding to the red dashed line in (a).

Fig. 2(b) presents the cross-section of the proposed device corresponding to the red dashed line in (a). The 50-nm thick slab region is doped by n+ type ion implantation. A 7 nm thick Al_2O_3 is deposited as gate dielectric material between the graphene layer and n+ type slab region. By applying the gate voltage V_g between the graphene layer and the n+ dope slab region, the Fermi level of the graphene can be tuned and the permittivity of the graphene can be changed. The real part and imaginary part of the permittivity under different Fermi levels [26] are shown in Fig. 3(a). The real part

peaks at E_f = 0.4 eV and the imaginary decreases if the Fermi level increases. Since the light in the silicon waveguide is evanescently coupled into the graphene layer, the variation of the permittivity has a strong influence on the effective index of the silicon-graphene hybrid waveguide. Fig. 3(b) shows the real part and the imaginary part of n_{eff} under different Fermi levels. Similarly as the trend of the permittivity, Re(n_{eff}) peaks at E_f = 0.4 eV and Im(n_{eff}) decreases if the Fermi level increases. And Re(n_{eff}) experiences an effective index change of 0.00164 if the Fermi level increases from 0.4 eV to 1 eV. Since Re(n_{eff}) determines the resonant wavelength of the nanobeam and Im(n_{eff}) determines the loss of the cavity, both the resonant wavelength and the quality factor of the cavity can thus be changed by tuning the Fermi level of the graphene.

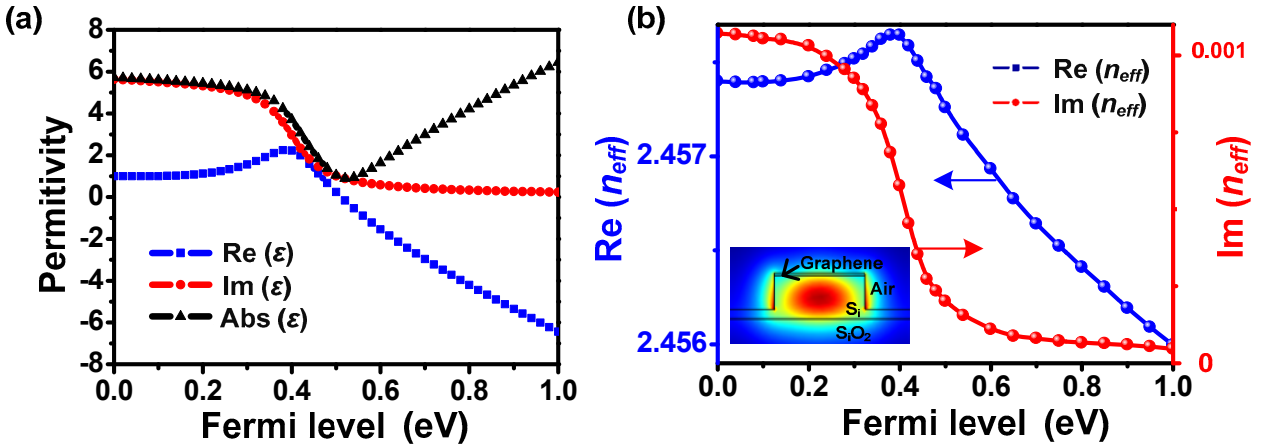

Figure 3 (a) Real part, imaginary part, and magnitude of the calculated anisotropic in-plane permittivity of graphene under different Fermi levels. (b) The real and imaginary parts of effective modal index of 500 × 220 nm^2 single-mode silicon waveguide with graphene on top as a function of the Fermi level. The inset is the electric field distribution profile of the TE mode. All the simulations are performed at an operation wavelength of 1550 nm.

FDTD simulations are performed to numerically analyze the performance of the device. As shown in Fig. 4(b), A FSR as large as 125.6 nm, a high ER of ~14 dB, and a relatively high Q-factor of ~5000 are achieved in our proposed device. Fig. 4(a) shows the transmission spectra under different Fermi levels. When the Fermi level is tuned from 0.4 eV to 0.9 eV, the modulation depth reaches about 12.5 dB if the input wavelength is set to be 1549.29 nm. The external applied voltage V_g used to tune the Fermi level of the graphene can be related to E_f by the formula [23]

$$E_f = \hbar V_f \sqrt{\pi (n_0 + \frac{C_p |V_g|}{q})} \quad ,$$

where C_p is the effective capacitance per unit area which is estimated to be ~20 mF/m^2 for the proposed device. $V_f = 10^6$ m/s is the Fermi velocity for the graphene, and $n_0 = 1.17 \times 10^{17}$ m^{-3} is the intrinsic carrier concentration. Thus a gate voltage V_g = 6.4 V is needed to shift E_f from 0.4 eV to 0.9 eV. The modulation speed of the proposed modulator is intrinsically determined by the RC time constant. It is calculated to be $1/2\pi RC$ = ~133 GHz if the contact resistance R is estimated to be ~20 Ω and the total capacitance C is assumed to be ~60 fF .

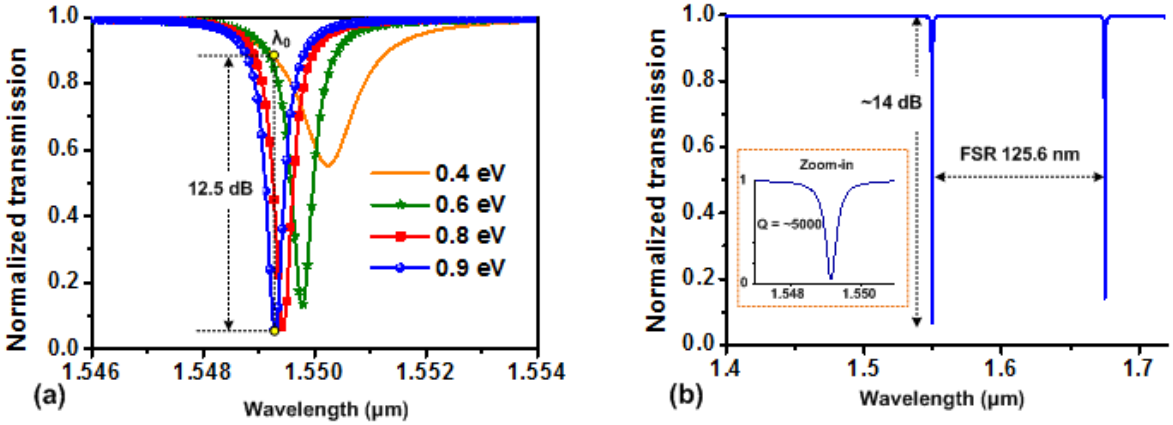

Figure.3. (a) Normalized transmission spectra of the proposed device at different Fermi levels. (b)Normalized transmission spectrum ranging from 1400 nm to 1670 nm at *Ef* = 0.9 eV. Inset shows zoom-in view of the spectrum ranging from 1545 nm to 1553 nm.

3.2 Micron-scale spatial light modulator valve (MSLV)

High-speed spatial light modulators (SLMs) could be useful in optical computing [27], optical tweezer [28] and switching in optical interconnetion. They are comprised generally of a spatial array of miniature, independent, electrically addressed pixels, where each pixel is a micron-scale spatial light valve (MSLV). Here we propose a new type of MSLV which is two orders faster than previous demonstrated one [9]. The schematic view of the device is shown in Fig .4(a) [24]. It consists of 1D photonic crystal cavity with the graphene layer on top. Detail device parameters can be found in the Ref [24]. Based on the diffraction coupling scheme, normal incident light can be coupled into the cavity [24]. Since the Fermi level of the graphene can be tuned based on capacitor structure as discussed above, the resonant wavelength and the loss of the cavity can be controlled. Based on 2D FDTD solution, the transmission spectra of the device under different Fermi levels are analyzed as shown in Fig. 3(b). If one sets the input wavelength to be λ_L = 1559.466 nm, more than 10 dB modulation depth can be obtained if the Fermi level is tuned from 0.4 eV to 0.8 eV. The gate voltage V_g is 4.8 V in order to shift the Fermi level from 0.4 eV 0.8 eV. The capacitance of the device is about 0.1 pF. Thus the speed of the device is estimated to be 45 GHz by assuming R of 30 Ω.

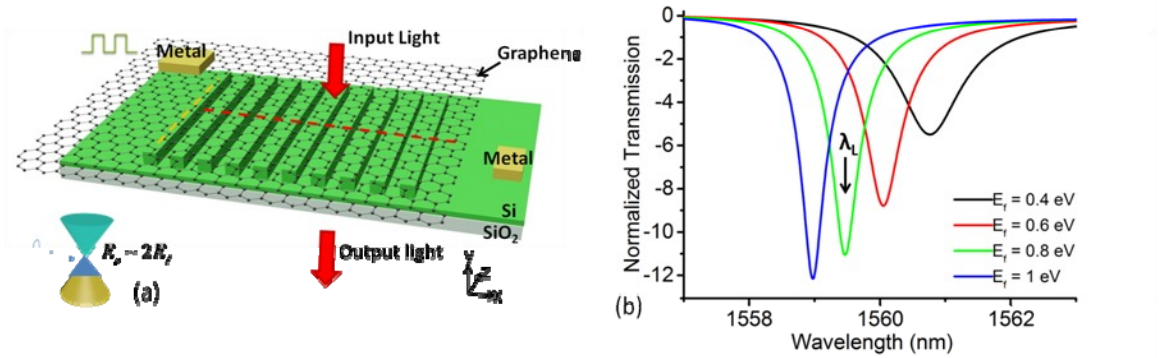

Figure.4(a). Diagram of the MSLV design in which the graphene is located on top of a silicon 1D PhC cavity (b)Transmission spectra under different Fermi levels from FDTD simulations. The width perturbation (Δ*w*) for this device is 10 nm.

4. CONCLUSIONS

We present light emitters and modulators for potential silicon photonic interconnects. We experimentally demonstrate resonant luminescence from Ge quantum dots embedded in a PCRR at room temperature. Six sharp resonant peaks, which correspond to the resonant modes supported by the PCRR, are observed to dominate the spectrum over an almost flat and weak background emission in the PL spectrum of the PCRR. We also propose a high speed silicon-graphene nanobeam modulator, and a silicon spatial light modulator. Based on FDTD simulations, their modulation speeds are expected to be higher than 45 GHz and their modulation depths are larger than 10 dB. These devices show great promise in future high density and high capacity interconnection systems.

REFERENCES

[1] D. Mahgerefteh and C. Thompson, "Techno-economic comparison of silicon photonics and multimode VCSELs" Proc. OFC Paper M3B.2, 934-937 (2015).

[2] R. Soref, "Silicon photonics: a review of recent literature," Silicon **2**(1), 1-6 (2010).

[3] M. Wang, X. Huang, J. Xu, W. Li, Z. Liu, and K. Chen, "Observation of the size-dependent blueshifted electroluminescence from nanocrystalline Si fabricated by KrF excimer laser annealing of hydrogenated amorphous silicon/amorphous-SiNx:H superlattices," Appl. Phys. Lett. **72**(6), 722-724 (1998).

[4] J. Xia, Y. Ikegami, K. Nemoto, and Y. Shiraki, "Observation of whispering-gallery modes in Si microdisks at room temperature," Appl. Phys. Lett. **90**(14), 141102 (2007).

[5] S. Nakayama, S. Ishida, S. Iwamoto, and Y. Arakawa, "Effect of cavity mode volume on photoluminescence from silicon photonic crystal nanocavities," Appl. Phys. Lett. **98**(17), 171102 (2011).

[6] A. Shakoor, R. Lo Savio, P. Cardile, S. L. Portalupi, D. Gerace, K. Welna, S. Boninelli, G. Franzò, F. Priolo, and T. F. Krauss, "Room temperature all ‐ silicon photonic crystal nanocavity light emitting diode at sub ‐ bandgap wavelengths," Laser & Photonics Reviews **7**(1), 114-121 (2013).

[7] W. Yue, Z. Jiashun, W. Yuanda, A. Junming, L. Jianguang, W. Hongjie, and H. Xiongwei, "Light Emission Enhancement From Er-Doped Silicon Photonic Crystal Double-Heterostructure Microcavity," IEEE Photon. Technol. Lett. **24**(2), 110-112 (2012).

[8] J. Liu, X. Sun, D. Pan, X. Wang, L. C. Kimerling, T. L. Koch, and J. Michel, "Tensile-strained, n-type Ge as a gain medium for monolithic laser integration on Si," Opt. Express **15**(18), 11272-11277 (2007).

[9] Y. De Koninck, G. Roelkens, and R. Baets, "Design of a Hybrid III-V-on-Silicon Microlaser With Resonant Cavity Mirrors," IEEE Photon. J. **5**(2), 2700413 (2013).

[10] S. Fukatsu, H. Sunamura, Y. Shiraki, and S. Komiyama, "Phononless radiative recombination of indirect excitons in a Si/Ge type-II quantum dot," Appl. Phys. Lett. **71**(2), 258-260 (1997).

[11] T. Brunhes, P. Boucaud, S. Sauvage, F. Aniel, J.-M. Lourtioz, C. Hernandez, Y. Campidelli, O. Kermarrec, D. Bensahel, and G. Faini, "Electroluminescence of Ge/Si self-assembled quantum dots grown by chemical vapor deposition," Appl. Phys. Lett. **77**(12), 1822-1824 (2000).

[12] J. Xia, Y. Ikegami, Y. Shiraki, N. Usami, and Y. Nakata, "Strong resonant luminescence from Ge quantum dots in photonic crystal microcavity at room temperature," Appl. Phys. Lett. **89**(20), 201102 (2006).

[13] M. El Kurdi, X. Checoury, S. David, T. Ngo, N. Zerounian, P. Boucaud, O. Kermarrec, Y. Campidelli, and D. Bensahel, "Quality factor of Si-based photonic crystal L3 nanocavities probed with an internal source," Opt. Express **16**(12), 8780-8791 (2008).

[14] X. Xu, S. Narusawa, T. Chiba, T. Tsuboi, J. Xia, N. Usami, T. Maruizumi, and Y. Shiraki, "Silicon-Based Light-Emitting Devices Based on Ge Self-Assembled Quantum Dots Embedded in Optical Cavities," IEEE J. Sel. Top. Quantum Electron. **18**(6), 1830–1838 (2012).

[15] Y. Zhang, C. Zeng, D. Li, Z. Huang, K. Li, J. Yu, J. Li, X. Xu, T. Maruizumi, and J. Xia, "Enhanced 1524-nm Emission From Ge Quantum Dots in a Modified Photonic Crystal L3 Cavity," IEEE Photon. J. **5**(5), 4500607 (2013).

[16] X. Xu, T. Tsuboi, T. Chiba, N. Usami, T. Maruizumi, and Y. Shiraki, "Silicon-based current-injected light emitting diodes with Ge self-assembled quantum dots embedded in photonic crystal nanocavities," Optics Express **20**(13), 14714-14721 (2012).

[17] P. Dong, S. R. Liao, D. Z. Feng, H. Liang, D. W. Zheng, R. Shafiiha, C. C. Kung, W. Qian, G. L. Li, X. Z. Zheng, A. V. Krishnamoorthy, and M. Asghari, "Low V-pp, ultralow-energy, compact, high-speed silicon electro-optic modulator," Optics Express 17(25), 22484-22490 (2009).
[18] D. J. Thomson, F. Y. Gardes, J. M. Fedeli, S. Zlatanovic, Y. F. Hu, B. P. P. Kuo, E. Myslivets, N. Alic, S. Radic, G. Z. Mashanovich, and G. T. Reed, "50-Gb/s Silicon Optical Modulator," IEEE Photonics Technology Letters 24(4), (2012).
[19] R. A. Soref and B. R. Bennett, "Electrooptical Effects in Silicon," IEEE Journal of Quantum Electronics 23(1), 123-129 (1987).
[20] M. Liu, X. B. Yin, E. Ulin-Avila, B. S. Geng, T. Zentgraf, L. Ju, F. Wang, and X. Zhang, "A graphene-based broadband optical modulator," Nature 474(7349), 64-67 (2011).
[21] X. T. Gan, R. J. Shiue, Y. D. Gao, K. F. Mak, X. W. Yao, L. Z. Li, A. Szep, D. Walker, J. Hone, T. F. Heinz, and D. Englund, "High-Contrast Electrooptic Modulation of a Photonic Crystal Nanocavity by Electrical Gating of Graphene," Nano Letters 13(2), 691-696 (2013).
[22] C. Y. Qiu, W. L. Gao, R. Vajtai, P. M. Ajayan, J. Kono, and Q. F. Xu, "Efficient Modulation of 1.55 mu m Radiation with Gated Graphene on a Silicon Microring Resonator," Nano Letters 14(12), 6811-6815 (2014).
[23] T. Pan, C. Y. Qiu, J. Y. Wu, X. H. Jiang, B. Y. Liu, Y. X. Yang, H. Y. Zhou, R. Soref, and Y. K. Su, "Analysis of an electro-optic modulator based on a graphene-silicon hybrid 1D photonic crystal nanobeam cavity," Optics Express 23(18), 23357-23364 (2015).
[24] C. Y. Qiu, T. Pan, W. L. Gao, R. L. Liu, Y. K. Su, and R. Soref, "Proposed high-speed micron-scale spatial light valve based on a silicon-graphene hybrid structure," Optics Letters 40(19), 4480-4483 (2015).
[25] C. Y. Qiu, J. B. Chen, Y. Xia, and Q. F. Xu, "Active dielectric antenna on chip for spatial light modulation," Scientific Reports 2 (855),1-8 (2012).
[26] J. Kim, H. Son, D. J. Cho, B. S. Geng, W. Regan, S. F. Shi, K. Kim, A. Zettl, Y. R. Shen, and F. Wang, "Electrical Control of Optical Plasmon Resonance with Graphene," Nano Letters 12(11), 5598-5602 (2012).
[27] D. E. Tamir, N. T. Shaked, P. J. Wilson, and S. Dolev, "High-speed and low-power electro-optical DSP coprocessor," Journal of the Optical Society of America a-Optics Image Science and Vision 26(8), A11-A20 (2009).
[28] O. M. Marago, P. H. Jones, P. G. Gucciardi, G. Volpe, and A. C. Ferrari, "Optical trapping and manipulation of nanostructures," Nature Nanotechnology 8(11), 807-819 (2013).